ChemComm

COMMUNICATION

View Article Online
View Journal | View Issue

Cite this: *Chem. Commun.*, 2017, **53**, 9813

Received 10th July 2017,
Accepted 10th August 2017

DOI: 10.1039/c7cc05313d

rsc.li/chemcomm

An AIE-based fluorescent test strip for the portable detection of gaseous phosgene†

Huiting Xie,‡ Yinglong Wu,‡ Fang Zeng,* Junjie Chen and Shuizhu Wu*

An AIE-based fluorescent test strip (OPD-TPE-Py-2CN) for rapid and sensitive detection of gaseous phosgene was designed. The fluorescence changes from blue to green upon exposure to phosgene. And the detection limit (1.87 ppm) is lower than the "harmless" level of human response to acute phosgene exposure.

Phosgene, an industrial chemical intermediate, is a colourless and highly toxic gas. During World War I, it was used as a chemical weapon agent and was responsible for nearly 80% of the deaths that were caused by chemical weapons.[1,2] Phosgene can react with proteins in the pulmonary alveoli and cause damage, resulting in extremely harmful effects to the respiratory tract and lungs. In the case of excessive inhalation, people may suffer from pulmonary edema or pulmonary emphysema, sometimes even death.[3] Compared with other chemical weapon agents, like sarin, soman and tabun whose usage and production are rigorously regulated and prohibited by laws,[4] phosgene is easily available since it is extensively used in industry.[5] Moreover, phosgene is widely applied in many chemical processes, especially in the production of plastics and pesticides, thereby posing a serious threat to public health safety. Hence, it is of great importance to develop a sensitive, rapid and portable method for the detection of phosgene to guard against unexpected phosgene leakage in industry or its potential use by terrorists.

Several methods have been reported for the detection of phosgene, including electrochemical and gas chromatography techniques.[6,7] However, these conventional methods are often limited by high cost, poor portability, as well as the time-consuming and sophisticated procedures. In comparison, fluorescence techniques, as an alternative detection method, is drawing more attention nowadays due to its high sensitivity, convenience, low cost, and real-time response.[8–16] Besides, fluorescence techniques possess obvious advantages in quantitative analysis. Among them, ratiometric fluorescent probes can avoid external interference by intrinsic calibration based on two emission bands,[17–22] this is why ratiometric-mode sensing is more suitable for application in practical samples compared to the turn-on or turn-off modes.

A number of fluorescent probes for the detection of phosgene have been developed so far, which are all based on aggregation-caused quenching (ACQ) fluorophores.[4–7,23–27] Some of these sensors have been prepared as test strips for phosgene detection, but the ACQ fluorophores always suffer from reduction or even quenching of their fluorescence in solid samples thus decreasing the sensitivity of the sensing system. In contrast, aggregation-induced emission (AIE) fluorophores exhibit weak fluorescence in the solution state, but they are highly emissive due to the restriction of intramolecular rotation in the solid state.[28–38] Therefore, AIE fluorophores are more suitable for the preparation of portable solid-state test-strip sensing systems compared with the ACQ ones. On the other hand, compared with the solution-type sensors, solid-state sensors such as membrane or test-strip sensors are more convenient for portable point-of-use detection. In this study, we developed a portable ratiometric fluorescent probe on a paper strip to achieve qualitative and quantitative detection of gaseous phosgene. As shown in Fig. 1, we incorporated an *o*-phenylenediamine moiety and a malononitrile group into an AIE fluorophore tetraphenylethene (TPE) and constructed a phosgene-responsive probe, OPD-TPE-Py-2CN. In the presence of phosgene, *o*-phenylenediamine in the probe can react with phosgene to form a new structure, causing the change in fluorescence of the sensing system. As far as we know, this is the first test-strip sensing system for gaseous phosgene fabricated with AIE-based fluorophores. The test strip can detect gaseous phosgene in a ratiometric way with a detection limit of 1.87 ppm, which is lower than the "harmless" level of human response to acute phosgene exposure ($\sim$25 ppm min^{-1}).[4,23,27]

The AIE-based probe OPD-TPE-Py-2CN was synthesized *via* the synthetic routes shown in Scheme S1 (ESI†) and the compounds

---

State Key Laboratory of Luminescent Materials and Devices, College of Materials Science and Engineering, South China University of Technology, Guangzhou 510640, P. R. China. E-mail: mcfzeng@scut.edu.cn, shzhwu@scut.edu.cn; Fax: +86 20 22236262; Tel: +86 20 22236262

† Electronic supplementary information (ESI) available: Experimental section, synthetic route, ^{1}H NMR and mass spectra, absorption spectra, AIE behaviour, fluorescence lifetimes, and determination of the detection limit. See DOI: 10.1039/c7cc05313d

‡ These authors contributed equally to this work.

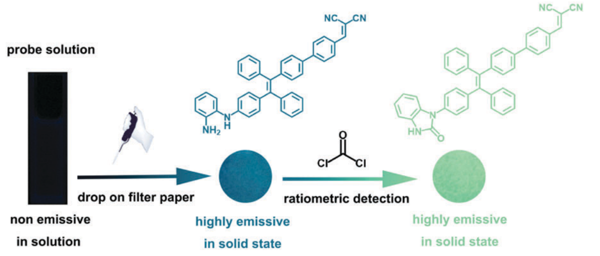

Fig. 1 Schematic illustration of the preparation of a test strip and its ratiometric fluorescence response towards phosgene. Photographs were taken under a 365 nm handheld UV lamp.

were characterized by using ^{1}H NMR and mass spectrometry (Fig. S1–S7, ESI†). Firstly, we studied the basic optical properties of the probe. The fluorescence quantum yield of our probe is 18.6%. The absorption spectrum of the probe is shown in Fig. S8 (ESI†). It can be seen that the probe has an absorption at 300–400 nm. Then we investigated the AIE properties of the probe. As shown in Fig. 2, OPD-TPE-Py-2CN is almost non-emissive in tetrahydrofuran (THF) solution. However, with the decline in the proportion of THF and the increase in the proportion of water, the fluorescence intensity of OPD-TPE-Py-2CN gradually increases, which could be explained by the fact that OPD-TPE-Py-2CN molecules start to form aggregates at a higher water fraction and this accordingly leads to the constraint of intramolecular motion thus activating the AIE process. In addition, from Fig. S9 (ESI†), we can see that the $I_{\text{solid}}/I_{\text{liquid}}$ ratio of OPD-TPE-Py-2CN at the emission peak is calculated to be 347. Compared with 4-bromotriphenylamine, a conventional ACQ fluorophore, $I_{\text{solid}}/I_{\text{liquid}}$ is only 0.175, which demonstrates that the AIE probe is highly emissive in the solid state while the ACQ fluorophore is quenched significantly in the solid state. As can be seen in Fig. S10 (ESI†), after the reaction with phosgene, the OPD-TPE-Py-2CN loaded test strips show intense fluorescence while there is hardly any fluorescence in solution because of the AIE properties of the probe. These phenomena further prove that AIE fluorophores are more promising for serving as fluorescent test strips.

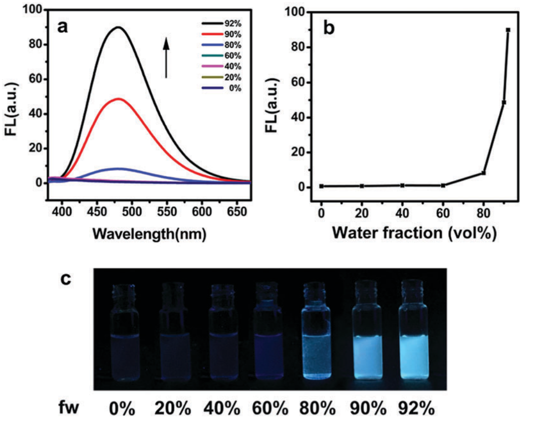

Fig. 2 (a) Fluorescence spectra of OPD-TPE-Py-2CN (10 μM) in the THF/water mixture (the percentage represents the water fraction); ex: 365 nm; (b) fluorescence intensity of OPD-TPE-Py-2CN (10 μM) at 475 nm as a function of water fraction under 365 nm excitation. (c) Photographs of OPD-TPE-Py-2CN in the THF/water mixture under 365 nm UV light (fw represents the water fraction).

In addition, the storage stability of the test strips was also investigated. The results are shown in Fig. S11 (ESI†). It can be seen that upon storage under continuous exposure to daylight, there is basically no obvious fluorescence intensity loss. This observation indicates that the system has good stability and holds great potential to act as a portable test strip.

Next we investigated the response of the probe on a test strip towards gaseous phosgene. When exposed to 64 ppm phosgene at 25 °C, the response time is fairly short, as can be seen from Fig. 3a and b. The fluorescence intensity ratio I_{496}/I_{435} reaches the maximum level in just 2 min, indicating the reaction between OPD-TPE-Py-2CN and phosgene reaches the equilibrium. Then we monitored the fluorescence changes of the probe loaded test strips exposed to different concentrations of phosgene at 25 °C and the results are shown in Fig. 3c and d. In the absence of phosgene, the test strip shows blue emission centered around 475 nm. Upon exposure to phosgene, the emission peak red-shifts to 496 nm. Meanwhile, the fluorescence changes from blue to green. With the increase in phosgene level, the fluorescence intensity of the reaction product around 496 nm gradually enhances along with the decrease in fluorescence intensity around 435 nm. Therefore, the probe loaded test strips can detect phosgene in a ratiometric mode. We chose five points of a dried aggregation spot on a Whatman filter paper and tested their fluorescence responses, as shown in Fig. S12 (ESI†). It is clear that

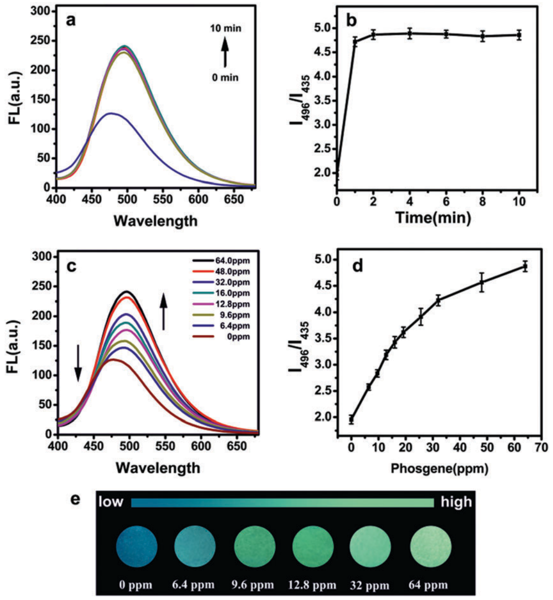

Fig. 3 (a) Time-dependent emission spectra and (b) fluorescence intensity ratio of OPD-TPE-Py-2CN loaded test strips in the presence of 64 ppm phosgene as a function of time. (c) Fluorescence spectra of OPD-TPE-Py-2CN loaded test strips in the presence of different phosgene concentrations for 2 min and (d) fluorescence intensity ratio as a function of phosgene concentration. Excitation wavelength: 365 nm. (e) Photographs of OPD-TPE-Py-2CN loaded test strips treated with different phosgene concentrations for 2 min at 25 °C taken under a 365 nm handheld UV lamp.

the fluorescence responses of different places of the dried aggregation spot on the Whatman filter paper show little difference. The fluorescence responses throughout the dried aggregation spot on the Whatman filter paper are basically uniform. And the detection limit for phosgene was determined to be 1.87 ppm (Fig. S13, ESI†). The fluorescence spectrum and photograph of the test strip after exposure to 1.87 ppm phosgene are shown in Fig. S14 (ESI†). Besides, in order to observe directly, we took photographs for the test strips under a 365 nm hand-held UV lamp. These test strips had been exposed to phosgene of different concentrations beforehand. From Fig. 3e we can see that the test strips exhibited blue fluorescence originally. After exposure to phosgene, the fluorescence gradually changes from blue to green. These visible changes make it highly promising for development into a portable on-site detector for gaseous phosgene.

To confirm the high selectivity of the OPD-TPE-Py-2CN test strip for the detection of phosgene, the fluorescence response of our probe towards other analytes, including diethyl chlorophosphate (DCP), thionyl chloride ($SOCl_2$), oxalyl chloride ($(COCl)_2$), sulfuryl chloride (SO_2Cl_2), phosphorus oxychloride ($POCl_3$), acetyl chloride (CH_3COCl) and tosyl chloride (TsCl), were investigated in parallel under the same experimental conditions. The overall fluorescence changes of OPD-TPE-Py-2CN are shown in Fig. 4a and c. The fluorescence intensity ratio I_{496}/I_{435} changes little with the addition of other analytes except phosgene and only the fluorescence of the test strips exposed to phosgene vapor changes from blue to green. The significant difference in fluorescence resulting from the exposure to phosgene and other analytes ensures low interference for detection. When treated with phosgene and other analytes simultaneously, as can be seen in Fig. 4b and d, the fluorescence changes and the I_{496}/I_{435} ratio remain nearly equivalent to those of the OPD-TPE-Py-2CN test strip in the presence of only phosgene, indicating that the co-existence of these analytes has no interference on phosgene detection. Besides, as can be seen in Fig. S15 (ESI†), when at a lower concentration (12.8 ppm), which is below the regulatory limit, the probe is still quite sensitive and selective for the detection of phosgene. And the co-existence of other analytes has little interfering effect on phosgene detection.

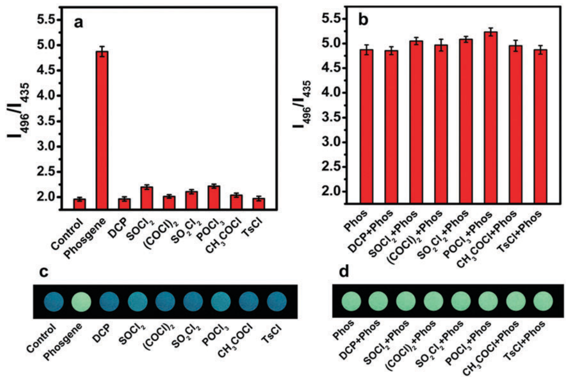

Fig. 4 Fluorescence intensity ratio (I_{496}/I_{435}) of OPD-TPE-Py-2CN loaded test strips (a) upon exposure to 64 ppm phosgene or DCP, $SOCl_2$, $(COCl)_2$, SO_2Cl_2, $POCl_3$, CH_3COCl, or TsCl at equal amounts, respectively, and (b) upon exposure to 64 ppm phosgene, simultaneously in the presence of DCP, $SOCl_2$, $(COCl)_2$, SO_2Cl_2, $POCl_3$, CH_3COCl or TsCl, respectively. The fluorescence intensities were measured 2 min after exposure. Excitation wavelength: 365 nm. Photographs of OPD-TPE-Py-2CN loaded test strips upon (c) exposure to 64 ppm phosgene or DCP, $SOCl_2$, $(COCl)_2$, SO_2Cl_2, $POCl_3$, CH_3COCl, or TsCl at equal amounts, respectively, and (d) exposure to 64 ppm phosgene, simultaneously in the presence of DCP, $SOCl_2$, $(COCl)_2$, SO_2Cl_2, $POCl_3$, CH_3COCl or TsCl, respectively; the fluorescence intensities were taken under 365 nm handheld UV light (Phos in this figure represents phosgene).

This detection method employs a phosgene-specific cyclization reaction of OPD-TPE-Py-2CN which contains an *o*-phenylenediamine moiety. When exposed to phosgene, the phenylenediamine group of OPD-TPE-Py-2CN can react with phosgene to form a ring structure. The probe displayed blue fluorescence originally. However, the fluorescence changes from blue to green when phosgene is present because the extent of the electronic push–pull effect varies. The proposed response mechanism was confirmed by MS and ^1H NMR experiments. As shown in Fig. S16 (ESI†), the molecular ion peak of the reaction product is located at *m*/*z* 617.1, which corresponds to the molecular weight of the predicted reaction product.

From ^1H NMR spectra (Fig. S17, ESI†), we can see that the proton peak of the primary amine shifts from 8.2 to 9.6 after the reaction. In addition, the absorption spectra before and after the reaction were obtained. As can be seen in Fig. S9 (ESI†), the maximum absorption of the reaction product red-shifts compared with that of the probe molecule. Besides, we measured the lifetimes of OPD-TPE-Py-2CN and the reaction product as well (Fig. S18, ESI†). The lifetimes of OPD-TPE-Py-2CN were 0.90 ns and 2.85 ns at 475 nm while those of the reaction product at 496 nm were 0.85 ns and 3.25 ns.

The comparisons of the reported probes for phosgene with the probe herein are shown in Tables S1 and S2 (ESI†). The probe herein is the first test-strip sensing system for gaseous phosgene fabricated with AIE-based fluorophores. Compared with ACQ-based fluorophores, which will exhibit fluorescence quenching at high concentrations or in the aggregated state, AIE-based fluorophores are more advantageous for development into solid sensors to detect gaseous phosgene. From the practical point of view, solid sensors are more suitable to detect phosgene because the gaseous phosgene in the air is difficult to get into solution and solid detection systems are conducive to portable point-of-interest application as well as visual detection.

In summary, we have successfully developed an AIE-based method to detect gaseous phosgene. The test strips with OPD-TPE-Py-2CN were fabricated to achieve a portable sensing approach for phosgene in the gas phase. As the first AIE-based solid sensor for phosgene detection, our test strips can effectively avoid the drawbacks of the aggregation-caused quenching phenomenon. The detection limit is 1.87 ppm, which is low enough to meet the safety requirements for public health. Moreover, the test strips can eliminate most interferences by realizing phosgene detection in a ratiometric mode. As for the probe, after the reaction with phosgene, the emission red shifts, along with the change in fluorescence from blue to green. Our strategy herein may present some helpful insights for developing convenient solid-state ratiometric fluorescence sensors and provide a portable method for the detection of gaseous phosgene.

We gratefully acknowledge the financial support from NSFC (21574044, 21474031 and 51673066), the Science and Technology Planning Project of Guangzhou (Project No. 201607020015), the Natural Science Foundation of Guangdong Province (2016A030312002), the Fundamental Research Funds for the Central Universities (2015ZY013) and Special Funds for the Cultivation of Guangdong College Students' Scientific and Technological Innovation (pdjh2017a0029).

Conflicts of interest

There are no conflicts to declare.

Notes and references

1 W. Li, F. Liu, C. Wang, H. Truebel and J. Pauluhn, *Toxicol. Sci.*, 2013, **131**, 612.
2 J. Beheshtian, A. A. Peyghan and Z. Bagheri, *Sens. Actuators, B*, 2012, **171–172**, 846.
3 W. W. Holmes, B. M. Keyser, D. C. Paradiso, R. Ray, D. K. Andres, B. J. Benton, C. C. Rothwell, H. M. Hoard-Fruchey, J. F. Dillman, A. M. Sciuto and D. R. Anderson, *Toxicol. Lett.*, 2016, **244**, 8.
4 H. C. Xia, X. H. Xu and Q. H. Song, *ACS Sens.*, 2017, **2**, 178.
5 P. Kundu and K. C. Hwang, *Anal. Chem.*, 2012, **84**, 4594.
6 H. Zhang and D. M. Rudkevich, *Chem. Commun.*, 2007, 1238.
7 X. Wu, Z. Wu, Y. Yang and S. Han, *Chem. Commun.*, 2012, **48**, 1895.
8 X. P. He, Y. Zang, T. D. James, J. Li, G. R. Chen and J. Xie, *Chem. Commun.*, 2017, **53**, 82.
9 X. Sun, J. S. Fossey, W. Zhai and T. D. James, *Chem. Commun.*, 2017, **52**, 3456.
10 J. Ding, H. Li, C. Wang, J. Yang, Y. Xie, Q. Peng, Q. Li and Z. Li, *ACS Appl. Mater. Interfaces*, 2015, **7**, 11369.
11 P. Li, L. Liu, H. Xiao, W. Zhang, L. Wang and B. Tang, *J. Am. Chem. Soc.*, 2016, **138**, 2893.
12 Y. Wu, J. Wang, F. Zeng, S. Huang, J. Huang, H. Xie, C. Yu and S. Wu, *ACS Appl. Mater. Interfaces*, 2016, **8**, 1511.
13 S. Kaur, V. Bhalla, V. Vij and M. Kumar, *J. Mater. Chem. C*, 2014, **2**, 3936.
14 C. Yu, M. Luo, F. Zeng, F. Zheng and S. Wu, *Chem. Commun.*, 2011, **47**, 9086.
15 S. Huang, Y. Wu, F. Zeng, L. Sun and S. Wu, *J. Mater. Chem. C*, 2016, **4**, 10105.
16 Y. Huang, P. Zhang, M. Gao, F. Zeng, A. Qin, S. Wu and B. Z. Tang, *Chem. Commun.*, 2016, **52**, 7288.
17 S. Pramanik, V. Bhalla and M. Kumar, *ACS Appl. Mater. Interfaces*, 2014, **6**, 5930.
18 F. Zheng, S. Guo, F. Zeng, J. Li and S. Wu, *Anal. Chem.*, 2014, **86**, 9873.
19 J. Du, B. Zhu, X. J. Peng and X. D. Chen, *Small*, 2014, **10**, 3461.
20 C. Yu, Y. Wu, F. Zeng and S. Wu, *J. Mater. Chem. B*, 2013, **1**, 4152.
21 Y. Wu, S. Huang, F. Zeng, J. Wang, C. Yu, J. Huang, H. Xie and S. Wu, *Chem. Commun.*, 2015, **51**, 12791.
22 C. Yu, X. Li, F. Zeng, F. Zheng and S. Wu, *Chem. Commun.*, 2013, **49**, 403.
23 Y. Zhang, A. Peng, X. Jie, Y. Lv, X. Wang and Z. Tian, *ACS Appl. Mater. Interfaces*, 2017, **9**, 1320.
24 X. Zhou, Y. Zeng, C. Liyan, X. Wu and J. Yoon, *Angew. Chem., Int. Ed.*, 2016, **55**, 4729.
25 S. L. Wang, L. Hong and Q. H. Song, *Chem. Commun.*, 2017, **53**, 1530.
26 Y. Hu, L. Chen, H. Jung, Y. Zeng, S. Lee, K. M. K. Swamy, X. Zhou, M. H. Kim and J. Yoon, *ACS Appl. Mater. Interfaces*, 2016, **8**, 22246.
27 H. C. Xia, X. H. Xu and Q. H. Song, *Anal. Chem.*, 2017, **89**, 4192.
28 X. Gao, G. Feng, P. N. Manghnani, F. Hu, N. Jiang, J. Liu, B. Liu, J. Z. Sun and B. Z. Tang, *Chem. Commun.*, 2017, **53**, 1653.
29 L. Yan, Y. Zhang, B. Xu and W. Tian, *Nanoscale*, 2016, **8**, 2471.
30 H. Wang, D. Chen, Y. Zhang, P. Liu, J. Shi, X. Feng, B. Tong and Y. Dong, *J. Mater. Chem. C*, 2015, **3**, 7621.
31 Y. Gao, Y. Qu, T. Jiang, H. Zhang, N. He, B. Li, J. Wu and J. Hua, *J. Mater. Chem. C*, 2014, **2**, 6353.
32 W. Zhang, Y. Chen, Y. Shao and L. J. Fan, *J. Mater. Chem. B*, 2014, **2**, 5249.
33 A. Shao, Y. Xie, S. Zhu, Z. Guo, S. Zhu, J. Guo, P. Shi, T. D. James, H. Tian and W. H. Zhu, *Angew. Chem., Int. Ed.*, 2015, **54**, 7275.
34 Z. Zhuang, Y. Tang, D. Ding, Y. Tsuchiya and Z. Zhao, *Chem. Commun.*, 2017, **53**, 3158.
35 Y. Bao, E. Guégain, V. Nicolas and J. Nicolas, *Chem. Commun.*, 2017, **53**, 4489.
36 H. Soleimaninejad, M. Z. Chen, X. Lou, T. A. Smith and Y. Hong, *Chem. Commun.*, 2017, **53**, 2874.
37 X. Liu and G. Liang, *Chem. Commun.*, 2017, **53**, 1037.
38 C. Yu, Y. Wu, F. Zeng, X. Li, J. Shi and S. Wu, *Biomacromolecules*, 2013, **14**, 4507.